

Classifying Mysterious Stellar Objects *via* Effective Temperature

Samuel English^{1,*}

¹*Department of Physics, University of California, Santa Cruz, CA 95064, USA*

(Dated: April 18, 2021)

The Dark Energy Camera (a part of the Blanco 4-m Dark Energy Survey telescope located in Chile), recently observed a set of three, unknown stars. Using foundational photometry methods, we decipher the classifications of these foreign bodies with the help of two, precisely-known, standard stellar objects. We find $C(\lambda)$, an apparatus-dependent constant, to have a weighted average of 25.07 ± 0.01 , 25.12 ± 0.01 , 25.13 ± 0.01 , and 25.10 ± 0.03 mag. between g , r , i , and z photometric bands. After converting to the Johnson system, we find each star's color ($B - V$) and subsequently effective temperature: 5220 ± 110 Kelvin (Harvard type G), 3180 ± 40 [K] (M), and 7040 ± 210 [K] (F), for Star 3, 4 & 5, respectively. This paper details the process of observation, implementation of automation, discussion of error propagation as well as results.

I. INTRODUCTION

Within the past month, the DECam (Dark Energy Camera, 2.2-degree diameter FOV, mounted on Cerro Tololo in Chile) has cataloged what are hypothesized to be unidentified stellar luminaries [1]. Originally designed for DES's access to supernova surveys and the wide-field, we attempt to classify a set of three potential star candidates from five observed [2] based on their respective spectral types. This would allow for further insight as to the true nature of these newcomer stars.







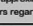
In this paper, we will discuss the theory behind observation IA and calculation of effective temperature IB; then, after discussing error analysis, we detail the procedure of obtaining our values II, present our results III, discuss the implications of our findings IIIB, as well as recap our findings and preview future work which could potentially expand upon what we've found IV.

A. Theoretics of Magnitude

Before we can analyze the FITS data for these objects, we must fully understand the workings behind converting the camera's observables to meaningful physicals.

To start, CCD's (Charged-Coupled Devices) operate by enacting a bias voltage across the semiconductor crystal, exposing it to a source of light, and measuring the resulting photo-current [3]. Thus, the data we receive from the CCD is particular to the number of counts N per pixel, proportional to the number of electrons stored in that pixel.

In order to convert the total number of counts N associated with a given star, we note that an image taken within the confines of some color filter is proportional to the photon flux F and the exposure time T as $N \propto FT$. More specifically, we can say that the visual magnitude

Spectral Type	Color	Temperature (K)*	Spectral Features
O		28,000-50,000	Ionized helium, especially helium
B		10,000-28,000	Helium, some hydrogen
A		7,500-10,000	Strong hydrogen, some ionized metals**
F		6,000-7,500	Hydrogen and ionized metals such as calcium and iron
G		5,000-6,000	Both metals and ionized metals, especially ionized calcium
K		3,500-5,000	Metals
M		2,500-3,500	Strong titanium oxide and some calcium

* To convert approximately to Fahrenheit, multiply by 9/5.
 ** Astronomers regard elements heavier than helium as metals.

Figure 1. Spectral type diagram (Harvard classification scheme), illustrates the qualities of a star's color & material features for a given temperature (Eugene R. Zizka).

of a star is related to its flux (w.r.t. Earth), by:

$$\begin{aligned} m(\lambda) &= -2.5 \log_{10}(F) + C(\lambda) \\ &= -2.5 \log_{10}\left(\frac{N}{T}\right) + C(\lambda) \end{aligned} \quad (1)$$

Here, T is known to be 90 seconds for all relevant images taken by the DECam and $C(\lambda)$ is a calibration constant (apparatus- & filter-dependent) which we will fix based on two other calibration stars with known visual magnitudes given in Tab. I.

Knowing $C(\lambda)$ to a high accuracy allows for the determination of the visual magnitude of each unknown star.

However, we must take caution when defining N , since extraneous signals can cause an overestimation of values. Therefore, before we obtain any $m(\lambda)$, we must correct for background noise using

$$\begin{aligned} M &= S + \left(B \frac{A_S}{A_B}\right) \\ S &= M - \left(B \frac{A_S}{A_B}\right) \end{aligned} \quad (2)$$

where M , the measured source signal, is the addition of S , the source counts within a region, with B , the back-

* sdenglis@ucsc.edu

ground counts within a separate region, attenuated by the ratio of $\frac{A_S}{A_B}$, the source to background region areas.

B. Filter Convention Conversion

All DECam images of stars are in the *ugriz* system, meaning that to calculate an effective temperature with known formulas, we must somehow convert between photometric systems. Thankfully, Jester et al. has already carried out an analysis of this process in detail [4] and found,

$$B - V = 0.98(g - r) + 0.22 \quad (3)$$

This now permits the calculation of any star's effective temperature given magnitudes in the *g* and *r* bands:

$$\begin{aligned} B - V &\approx \frac{7000}{T_{\text{eff}}} - 0.56 \\ T_{\text{eff}} &\approx \frac{7000}{(B - V) + 0.56} \end{aligned} \quad (4)$$

At the point that effective temperatures are known, one can easily classify each star by its Harvard spectral classification (see Fig. 1).

C. Error Propagation & Statistical Methods

The act of observation comes with various issues relating to accuracy. One needs to worry about the distortion of astronomical source due to the Earth's atmosphere, variations in intensity, position, sharpness. Even different layers and wave-fronts of the sky distort and attenuate the detector's influx of photons.

For simplicity, we are to assume that systematic variations between FITS images are more important than the statistical count errors in *N*, since the sampled background has decent statistics (i.e. $\sqrt{B} \ll B$).

We do, on the other hand, still have to juggle uncertainties propagated from the flux into the magnitude, moreover the error on $C(\lambda)$.

In order to propagate error, we utilize the general formula for error propagation, given the term we wish to isolate an uncertainty for $f(x_1, \dots, x_N)$:

$$\sigma_{x_i} = \sqrt{\sum_{i=1}^N \left(\frac{\partial f}{\partial x_i} \sigma_{x,i} \right)^2} \quad (5)$$

We are provided five images of each star in each filter of *griz*. Initially, given the above assumptions, we precipitate error from our flux $F = \frac{N}{T}$, where *N* is given by Eq. (2). Taking the mean and standard deviation of each filter's value array allows for propagation into $C(\lambda)$

for our first two standard candle stars:

$$\sigma_{C_i(\lambda)} = \sqrt{\left(\frac{2.5}{\ln(10)F_i} \sigma_{F_i} \right)^2} \quad (6)$$

With $i \in (1, 2)$, representing the calibration error for stars one and two. To get a better estimate on the calibration factor $C(\lambda)$ and its uncertainty, we simply take the weighted average as such:

$$\bar{C}(\lambda) = \sum_i \frac{C_i(\lambda)}{\sigma_i^2} \pm \sqrt{\frac{1}{\sum_i w_i}} \quad (7)$$

Here, $w_i = \frac{1}{\sigma_i^2}$. Now that we have the error in $\bar{C}(\lambda)$, we can look at the deviation for each of the unknown stars' visual magnitudes using Eq.'s (1) and (5):

$$\sigma_{m(\lambda)} = \sqrt{\left(\frac{2.5}{\ln(10)F} \sigma_F \right)^2 + \sigma_{\bar{C}(\lambda)}^2} \quad (8)$$

Again, using the same method of propagation, we find that the error in color (B-V) is given by

$$\sigma_{B-V} = \sqrt{(0.98\sigma_g)^2 + (-0.98\sigma_r)^2} \quad (9)$$

and subsequently the error in T_{eff} is

$$\sigma_T = \frac{7000}{((B - V) + 0.56)^2} \sigma_{B-V} \quad (10)$$

II. APPARATUS AND PROCEDURE

In conjunction with the Dark Energy Survey Collaboration, we used this state-of-the-art camera (DECam) consisting of a five-element, optical corrector, seven band filters, a CCD focal plane of 250- μm thick CCDs cooled within a vacuum Dewar [1], to observe unknown stars and determine their respective spectral types.

DECam outputs CCD information which is later condensed into a readable format such as FITS: our project begins with an archive dump of five stellar objects, each containing five FITS slices taken for the *g*, *r*, *i*, and *z* photometric bands.

Courtesy of the Astropy package photutils [5], we can easily mask elliptical shapes on the intensity pixel-grid to reproduce the visuals seen in Fig. 2 for every FITS file we feed it.

Upon inspection of the FITS images, we are less concerned with background than one might typically worry, due to the clear nature of the photographs. These stars are apparently bright, making it more likely to accidentally exclude some star flux rather than include too much background noise. In the bluer bands, we rightfully see the intensity of pixels smeared across wider radii, due to seeing effects (attributed to the Earth's atmosphere,

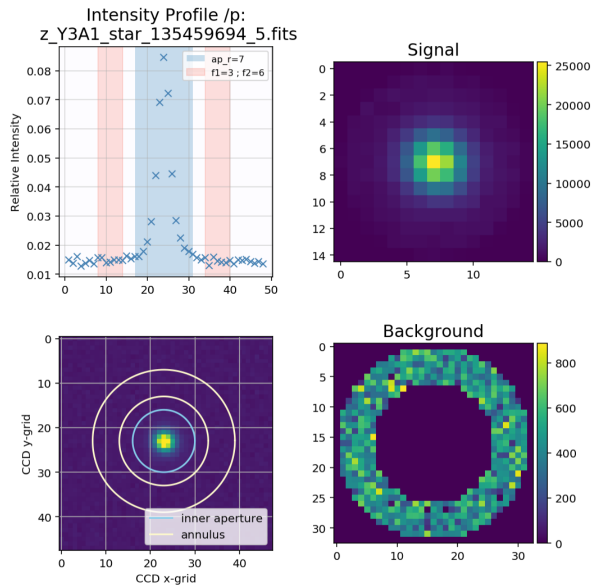


Figure 2. Star 1 in the z band (z.Y3A1_star135459694_5.fits). *Upper left*: the intensity profile for a given star. Each hash represents a flattened axis section from the original CCD image. *Lower left*: CCD image depicts pixel intensity of source star. Blue ring shows inner aperture cutoff, outer annulus is the background region. *Upper right*: 2-D signal histogram with signal count height. *Lower right*: 2-D histogram, but for background annulus & associated counts.

Star	g magnitude	r magnitude	i magnitude	z magnitude
Star 1	16.262	16.023	15.935	15.936
Star 2	17.806	16.459	15.850	15.524

Table I. Two standard stars with known magnitudes for each system band (sans u). Assumed to be baseline for significant digits given the lack of uncertainty on their magnitudes.

which causes noticeable shifts between bands and taken images). However, by increasing the aperture radius to a sufficiently large value, we can ensure the capture of the star’s observable flux.

Implementing an automated algorithm to process each star’s contents allows for the determination of our calibration factor $C(\lambda)$, observed flux F , visual magnitude $m(\lambda)$, $(B - V)$ color, and subsequently stellar temperature T_{eff} all within the confines of the uncertainty.

III. RESULTS AND DISCUSSION

A. Values for Analysis

Eq. (1), when solved for $C(\lambda)$, provides a simple method to incorporate Tab. I’s known values (for stars one & two) with the background-adjusted signal counts as depicted in Fig. 2. We quote the corrective factors in

$C(\lambda)$	Star 1	Star 2	Weighted Avg.
g mag.	25.01 ± 0.05	25.14 ± 0.03	25.07 ± 0.01
r mag.	25.09 ± 0.02	25.16 ± 0.02	25.12 ± 0.01
i mag.	25.04 ± 0.03	25.13 ± 0.01	25.13 ± 0.01
z mag.	25.04 ± 0.03	25.07 ± 0.01	25.10 ± 0.03

Table II. Determination of the calibration constant $C(\lambda)$ for each photometric band. Star 1 & 2 are taken to be standard stars; we take a simple weighted averaged between the two to obtain a realistic factor to apply to the leftover, unknown stars ($w_i = \frac{1}{\sigma_i^2}$).

Tab. II, noting that each subsequent value presented is limited by the significant figure count of the initial, standard candles. The weighted average between the two is taken, using the the inverse of the variance as weighting; we find a reasonable constant for each band to use in our subsequent analysis (25.07 ± 0.01 , 25.12 ± 0.01 , 25.13 ± 0.01 , and 25.10 ± 0.03 mag. for g , r , i , z bands, respectively).

Knowing $C(\lambda)$, we determine the visual magnitudes of the three unknown stars with the aid of Eq.’s (1) & (2); then, isolating both the g and r bands, we use Eq. (3) to calculate each star’s $(B - V)$ color alongside Eq. (4) to get their effective temperatures (Tab. III). To a modest degree of accuracy, we quote Star 3 as having an effective temperature of 5220 ± 110 Kelvin, Star 4 as 3180 ± 40 [K], with Star 5 at 7040 ± 210 [K].

B. Statistical Interpretation

Let’s first discuss the potential causes for the bi-modal nature of $C_1(\lambda)$ & $C_2(\lambda)$ combined. Ideally, these correctional factors would line up exactly for both of the recorded calibration stars; however this seems not to be the case. Tab. II tells a different story: the difference between the two compared with uncertainties illustrates that their errors are too small to overlap with discrepancies in range. While being a relatively small number, it is none-the-less entirely significant. This effect could potentially be attributed to the pesky atmosphere, observing conditions or seeing. Furthermore, we neglected to account for statistical errors in the number of counts, which could very well play a key role in this mismatching of values.

As for the continuation of our estimation, Tab. III yields insightful information on the types of stars we have observed. According to the Harvard star classification scheme depicted in Fig. 1, we can further inscribe physical meaning to the CCD results of the DECcam.

The third star, weighs in at an effective temperature of 5220 ± 110 [K]. This falls under the low-end spectral type G (Yellow supergiant), composed of both metals and ionized metals (heavily sourced with ionized calcium). This class of stars (including our sun [6]) have a yellowish-white chromacity (D65) [7], weak hydrogen lines, and

$m(\lambda)$	Star 3	Star 4	Star 5
g mag.	16.71 ± 0.03	17.99 ± 0.03	16.23 ± 0.03
r mag.	16.14 ± 0.01	16.53 ± 0.01	16.23 ± 0.01
i mag.	15.96 ± 0.01	15.90 ± 0.01	16.01 ± 0.01
z mag.	15.79 ± 0.01	15.55 ± 0.01	16.00 ± 0.01
$(B - V)$	0.78 ± 0.03	1.64 ± 0.03	0.43 ± 0.03
T_{eff} [K]	5220 ± 110	3180 ± 40	7040 ± 210

Table III. Visual magnitude $m(\lambda)$ in each photometric band ($griz$), $(B - V)$ color (as calculated using Eq. (3)), and effective temperature T_{eff} for each unknown star (Eq. (4)).

compose roughly 7.6% of all main-sequence stars [8].

The fourth star, 3180 ± 40 [K], is predicted to be spectral type M (Red dwarf, giant, supergiant): stars containing a strong amount of titanium oxide as well as some calcium. Typically with a light, orange-red chromacity (D65) [7] and very weak hydrogen lines, these stars contribute to around 76.45% of all main-sequence stars [8].

The fifth (and last) star, calculated to burn at an effective temperature of 7040 ± 210 [K], can safely be classified as a Harvard spectral type F . F-type stars (with white chromacity [7]), contain medium-strength hydrogen lines

(hydrogen and ionized metals such as iron and calcium make up the star), and compose only 3% of all main-sequence stars [8].

IV. CONCLUSIONS

We have shown that “DES0254+0043_r2674p01”, “DES2339+0043_r2587p01”, “DES2336-0041_r2587p01” (stars three, four, & five) can be categorized into Harvard spectral types G , M , and F , respectively.

Despite casting away any intrinsic statistical fluctuations in the data for simplicity, we still managed to get a handle on these stars. Using five-fold redundancy to determine the atmospheric variability (airmass, cloudiness), we found that Star 3 had an effective temperature of 5220 ± 110 Kelvin, Star 4, 3180 ± 40 [K], and Star 5, 7040 ± 210 [K].

All five of the observed stars using DECcam decam on the Blanco 4-m telescope as a part of the DES Collaboration [2] now have a solid, analytic foundation. We hope this work garners attention from others to cross-check our results and re-affirm the categorization of each unknown star.

ACKNOWLEDGMENTS

SE is a part of the ASTR 135, Advanced Laboratory course. None of this information is presented for journal publication, only for writing improvement.

BIBLIOGRAPHY

- [1] Flaugher et al., “The Dark Energy Camera”, The Astronomical Journal, 150, 150 (2015)
- [2] DES Collaboration, “The Dark Energy Survey”, white paper submitted to the Dark Energy Task Force, arXiv:astro-ph/0510346 (2005)
- [3] Rieke, George H.. Measuring the Universe : A Multiwavelength Perspective, Cambridge University Press, 2012.
- [4] Jester et al., “The Sloan Digital Sky Survey View of the Palomar-Green Bright Quasar Survey”, The Astronomical Journal, 130, 873 (2005).
- [5] <https://photutils.readthedocs.io/en/stable/>
- [6] Phillips, Kenneth J. H. (1995). Guide to the Sun. Cambridge University Press. pp. 47–53. ISBN 978-0-521-39788-9.
- [7] Moore, Patrick (1992). The Guinness Book of Astronomy: Facts Feats (4th ed.). Guinness. ISBN 978-0-85112-940-2.
- [8] Ledrew, Glenn (February 2001). ”The Real Starry Sky”. Journal of the Royal Astronomical Society of Canada. 95: 32. Bibcode:2001JRASC..95...32L.